13 NONLINEAR KINEMATIC HARDENING LAWS

In the previous chapter the problems with establishing a plasticity model that can predict an accurate response when significant reversed loadings occur were highlighted. A generalization of Melan-Prager's kinematic hardening law to account for nonlinear hardening behavior was discussed, and it was shown that the most natural assumptions lead to unrealistic behavior of the model, cf. Section 12.3. It was concluded that it is difficult to account for nonlinear hardening when Melan-Prager's kinematic hardening rule is used. In this chapter, other possibilities to model nonlinear kinematic hardening will be discussed and special emphasis will be given to the situation where the von Mises yield criterion is adopted.

The candidates considered in this exposition are the model of Mróz (1967), the so-called bounding surface models of Dafalias and Popov (1975, 1976) and Krieg (1975), and the nonlinear kinematic formulation of Armstrong and Frederick (1966). A review of these models is also provided by Khan and Huang (1995)

13.1 Mróz model

An intriguing model suitable when reversed loadings occur was proposed by Mróz (1967); somewhat similar models were proposed by Besseling (1953) and Iwan (1967). The *Mróz model* forms the basis of many more advanced models and we will therefore provide a detailed discussion of its ingredients.

For reasons previously discussed, kinematic hardening was restricted to linear hardening. The essential feature of the Mróz model is that the response of the material is approximated by a multilinear response and for each linear part of the response, a linear kinematic hardening model is adopted. For uniaxial loading, this idea is illustrated in Fig. 13.1; it appears that in each linear region, we have a constant plastic modulus, i.e.

$$H_n = \text{constant} \; ; \quad n = 0, 1, 2, \cdots$$

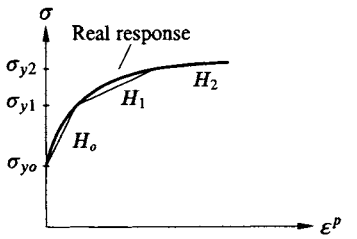

Figure 13.1: Multilinear approximation of uniaxial response with constant plastic moduli given by H_0, H_1,H_2,$\cdots$.

Figure 13.1 shows that between the constant stress values σ_{y0} and σ_{y1}, the plastic modulus is given by H_0 and between the constant stress values σ_{y1} and σ_{y2}, the plastic modulus is given by H_1, etc. We have

$$\sigma_{yn} = \text{constant} \; ; \quad n = 0, 1, 2, \cdots \tag{13.1}$$

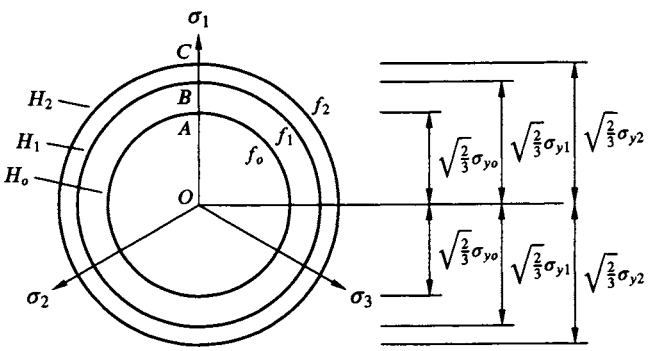

Figure 13.2: Position of von Mises surfaces in the deviatoric plane before any loading; regions with constant plastic moduli.

Within a von Mises concept, let us generalize these ideas to arbitrary stress states. We then envisage the following von Mises surfaces that all may be subjected to kinematic hardening

$$f_n = F_n - \sigma_{yn} = 0 \; ; \quad n = 0, 1, 2, \cdots \tag{13.2}$$

where the function F_n is defined by

$$F_n = [\frac{3}{2}(s_{ij} - \alpha_{ij}^{d(n)})(s_{ij} - \alpha_{ij}^{d(n)})]^{1/2} \; ; \quad n = 0, 1, 2, \cdots \tag{13.3}$$

and $\alpha_{ij}^{d(n)}$ denotes the deviatoric part of the back-stress belonging to the surface f_n with size σ_{yn}. Before any loading, all back-stresses $\alpha_{ij}^{d(n)}$ are zero and in the deviatoric plane, the surfaces f_n then take the form shown in Fig. 13.2 where

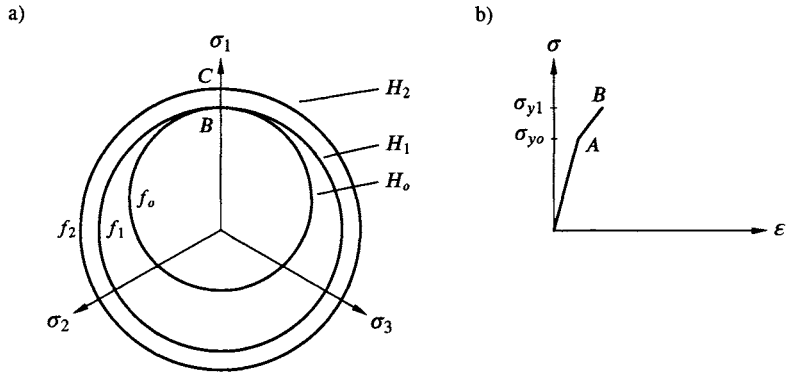

Figure 13.3: Increasing uniaxial loading; a) deviatoric plane, b) uniaxial response.

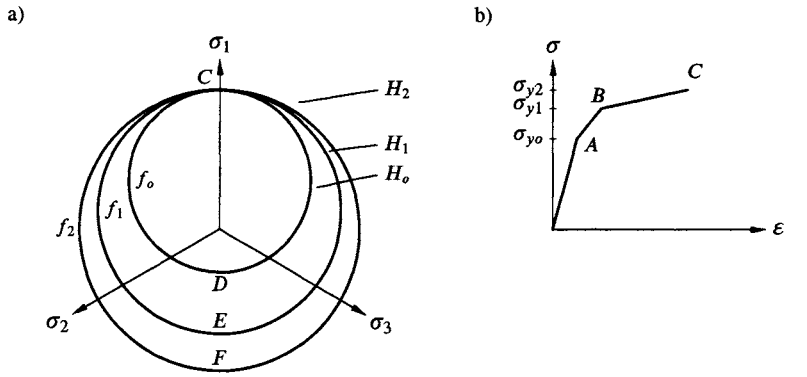

Figure 13.4: Increasing uniaxial loading; a) deviatoric plane, b) uniaxial response.

the radii are given by $\sqrt{2J_2} = \sqrt{\frac{2}{3}}\sigma_{yn}$, cf. (8.13). In the regions between the circles, different constant plastic moduli apply.

Referring to Fig. 13.2, let us now evaluate the model for uniaxial loading. When the stress point moves from the origin O along the vertical axis, it reaches the initial yield stress σ_{y0} at point A and the circle f_0 moves as a rigid body along this axis until it contacts and touches the circle f_1 at point B; all other circles remain fixed during this process and the situation when the stress has reached point B is shown in Fig. 13.3a). The corresponding stress-strain curve is shown in Fig. 13.3b) where it is recalled that between A and B, the plastic modulus is constant and given by H_0.

When the stress point moves from B towards C, the circles f_0 and f_1 translate together until point C is reached. At that state, f_0 and f_1 touch the circle f_2, which up until now remained at rest, cf. Fig. 13.4a). Between point B and

C, the plastic modulus is constant and given by H_1, i.e. we have the response shown in Fig. 13.4b). This type of process will continue for increased loading.

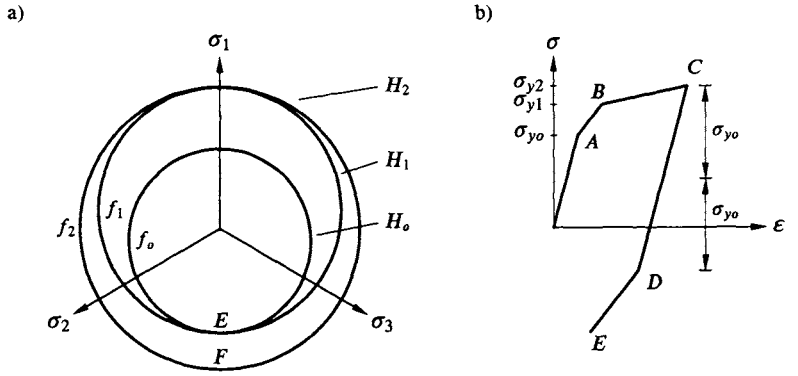

Figure 13.5: Reversed uniaxial loading; a) deviatoric plane, b) uniaxial response.

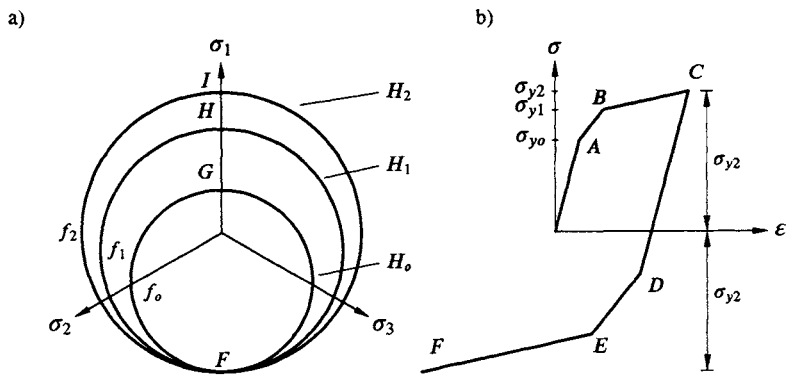

Figure 13.6: Reversed uniaxial loading; a) deviatoric plane, b) uniaxial response.

Consider now the process of reversed loading. When moving from point C towards point D, cf. Fig. 13.4a), an elastic response occurs. When the stress point reaches point D, the circle f_0 translates downwards until it reaches the circle f_1 at point E. This situation is shown in Fig. 13.5a) and since the plastic modulus between circle f_0 and f_1 is given by H_0, we have the same slope between D and E as between A and B, cf. Fig. 13.5b). Note that the stress difference between point D and E equals twice the stress difference between point A and B. When the stress point moves from point E towards F, cf. Fig. 13.5a), the two circles f_0 and f_1 move together and the relevant plastic modulus is now that applicable between circle f_1 and f_2, i.e. H_1. The situation where point F has been reached is shown in Fig. 13.6a) and the corresponding stress-strain

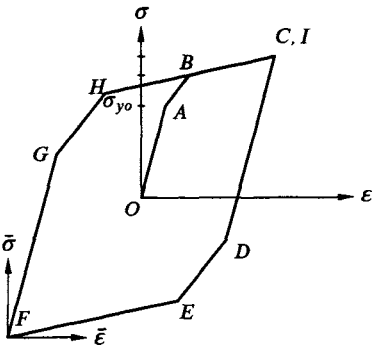

Figure 13.7: Reversed uniaxial response.

curve is given in Fig. 13.6b). Again the slope between E and F is the same as between B and C; moreover, the stress difference between E and F is twice the stress difference between B and C. At point F the stress is $\sigma = -\sigma_{y2}$ and it is recalled that at point C the stress is $\sigma = \sigma_{y2}$. Since the stress difference between $C-D$, $D-E$ and $E-F$ is twice the difference between $O-A$, $A-B$ and $B-C$, respectively, the strains at point F and at point C are related by $\varepsilon_F = -\varepsilon_C$.

When we reverse the loading from point F, cf. Figs. 13.6 and 13.7, the process is repeated, i.e. FG, GH and HI corresponds to CD, DE and EF, respectively; therefore, point I will coincide with point C. Let us next locate a $\bar{\sigma}\bar{\varepsilon}$–coordinate system at point F, cf. Fig. 13.7. It is then apparent that if the stress-strain curve $OABC$ is described by $\sigma = f(\varepsilon)$, then the curve $FGHI$ is described by

$$\boxed{\frac{1}{2}\bar{\sigma} = f(\frac{1}{2}\bar{\varepsilon}) \; ; \quad \textit{Masing's rule}} \tag{13.4}$$

This expression corresponds to the so-called *Masing's rule* and as observed by Masing (1927) it provides a fairly close approximation to the real behavior of metals and steel. If we now reverse the loading from point C, we will again follow path $CDEF$ and it is apparent that Fig. 13.7 corresponds both to symmetric stress cycling and symmetric strain cycling; it appears that no cyclic hardening or softening effects are predicted, cf. Figs. 12.2 and 12.3, and the stabilized cyclic stress-strain curve is obtained already after one cycle. However, the predicted response during reversed loading is much closer to the real behavior of metals and steel than that predicted by the previous models.

Consider the bar consisting of the three layers, cf. Fig. 13.8; each layer is assumed to exhibit a perfectly plastic response. As all layers undergo the same deformation, it is evident that the response in uniaxial loading will be identical to that shown in Fig. 13.7 and this forms the basis for the *sublayer models* proposed by Besseling (1953) as well as by Iwan (1967). It was also used by Masing (1927) to derive relation (13.4).

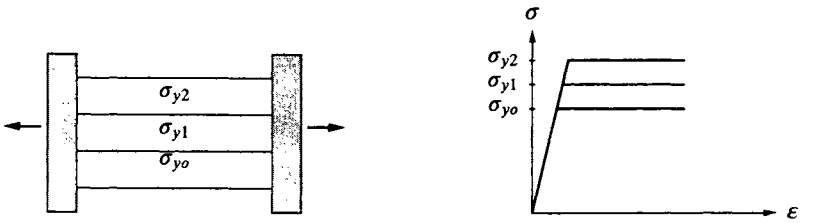

Figure 13.8: Sublayer model also resulting in the response shown in Fig. 13.7.

We will now see how the concepts above can be generalized to arbitrary non-proportional loading. We will also allow the yield functions to be written in the quite general form

$$\boxed{\begin{aligned} &f_n = F_n - (\sigma_{yn})^p = 0 \ ; \quad n = 0, 1, 2, \cdots \\ &\textit{where} \quad F_n = F(\sigma_{ij} - \alpha_{ij}^{(n)}) \end{aligned}} \tag{13.5}$$

As usual, the parameters σ_{yn} have the dimension of stress. To ensure that F_n and $(\sigma_{yn})^p$ possess the same dimension, the function F is required to be a *homogeneous function of degree p* in the variables $\sigma_{ij} - \alpha_{ij}^{(n)}$. This means that for any number 'a' we have

$$\boxed{F(a(\sigma_{ij} - \alpha_{ij}^{(n)})) = a^p F(\sigma_{ij} - \alpha_{ij}^{(n)}) \ ; \quad n = 0, 1, 2, \cdots} \tag{13.6}$$

cf. for instance Sokolnikoff and Redheffer (1958) p.234. As an example, in the von Mises case where F is given by (13.3), F is a homogeneous function of degree one; in that case $p = 1$ and (13.5) reduces to (13.2).

In the general stress space, the active yield surface f_n is moving and the next yield surface f_{n+1} is fixed in the stress space, cf. Fig. 13.9. Here point O is the origin of the stress space, O_n is the center of the active yield surface f_n and O_{n+1} is the center of the next yield surface f_{n+1}.

The problem we are facing is to devise a rule for how the surface f_n is moving, i.e. we have to identify the evolution law for $\dot{\alpha}_{ij}^{(n)}$. For this purpose, the following two criteria are used:

- The active surface f_n is not allowed to intersect the surface f_{n+1} at any point. At contact, the smaller surface f_n must therefore touch the larger surface f_{n+1} tangentially.

- After tangential contact has been established, the two surfaces move together and approach the next surface f_{n+2}. The two surfaces f_n and f_{n+1} are detached only after elastic unloading and subsequent plastic reloading in a new direction.

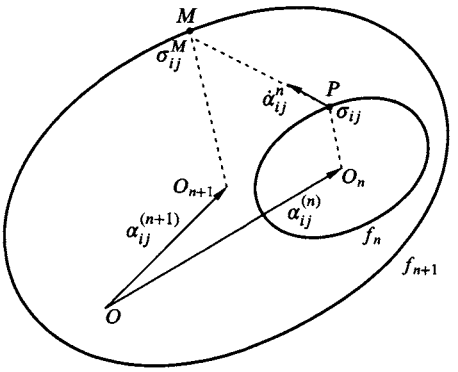

Figure 13.9: Stress space illustrating the general situation; f_n = active yield surface, f_{n+1} = next yield surface.

The notion of *nesting yield surfaces* is often used in connection with the Mróz model and this terminology hinges on the fulfillment of the criteria just discussed. Before the evolution law for $\dot{\alpha}_{ij}^{(n)}$ can be identified, some preliminary results shall be established.

Suppose that the current stress state σ_{ij} is located at point P, cf. Fig. 13.9. Define next a stress state σ_{ij}^M located on the surface f_{n+1} at point M such that the vector $O_{n+1}M$ is parallel with the vector O_nP. This means that

$$\boxed{\sigma_{ij}^M - \alpha_{ij}^{(n+1)} = a(\sigma_{ij} - \alpha_{ij}^{(n)}) \; ; \quad a > 1} \tag{13.7}$$

where a is some proportionality factor larger than one. For reasons that will become apparent in a moment, σ_{ij}^M is called the *image stress* or *mapping stress*. To determine the factor a present in (13.7), we take that the mapping point M is located on the yield surface f_{n+1} whereas the the current stress point P is located on the active surface f_n. From (13.5), we then obtain

$$\frac{F(\sigma_{ij}^M - \alpha_{ij}^{(n+1)})}{F(\sigma_{ij} - \alpha_{ij}^{(n)})} = (\frac{\sigma_{y(n+1)}}{\sigma_{yn}})^p \tag{13.8}$$

Moreover, (13.7) and (13.6) give

$$F(\sigma_{ij}^M - \alpha_{ij}^{(n+1)}) = a^p F(\sigma_{ij} - \alpha_{ij}^{(n)}) \tag{13.9}$$

Insertion into (13.8) provides

$$\boxed{a = \frac{\sigma_{y(n+1)}}{\sigma_{yn}}} \tag{13.10}$$

With this result, (13.7) determines the mapping stress σ_{ij}^M uniquely.

Intuitively, and referring to Fig. 13.9, it appears that the normal to the surface f_{n+1} at point M and the normal to the surface f_n at point P are parallel. To prove this formally, we observe that (13.7) and (13.10) imply that to each stress σ_{ij} on the surface f_n there exists a stress σ_{ij}^M on the surface f_{n+1}. From (13.5), (13.9) and (13.7), we then have

$$\frac{\partial f_{n+1}}{\partial \sigma_{ij}^M} = a^p \frac{\partial F(\sigma_{st} - \alpha_{st}^{(n)})}{\partial \sigma_{kl}} \frac{\partial \sigma_{kl}}{\partial \sigma_{ij}^M} = a^{p-1} \frac{\partial F(\sigma_{st} - \alpha_{st}^{(n)})}{\partial \sigma_{ij}}$$

Moreover, (13.5) gives

$$\frac{\partial f_n}{\partial \sigma_{ij}} = \frac{\partial F(\sigma_{st} - \alpha_{st}^{(n)})}{\partial \sigma_{ij}}$$

It appears that

$$\frac{\partial f_{n+1}}{\partial \sigma_{ij}^M} = a^{p-1} \frac{\partial f_n}{\partial \sigma_{ij}} \tag{13.11}$$

i.e. the normals at point M and at point P are parallel.

Referring to Fig. 13.9, we then conclude that if $\dot{\alpha}_{ij}^{(n)}$ is always directed from the current stress point P towards the corresponding mapping point M, then the two surfaces will contact each other at the mapping point M. On contact, the current stress point P and the mapping point M coincide. Since the normals at point P and at point M are parallel, this contact will occur tangentially without any intersection of the two surfaces. We are then led to the *kinematic evolution law of Mróz* that reads

$$\boxed{\dot{\alpha}_{ij}^{(n)} = \dot{\lambda}\, q(\sigma_{ij}^M - \sigma_{ij}) \;; \quad \textit{evolution law of Mróz}} \tag{13.12}$$

where q is a positive quantity. To be precise, Mróz (1967) did not introduce the plastic multiplier $\dot{\lambda}$ at this point. However, in order to be consistent with the theoretical framework adopted here, we will deviate somewhat from the exposition by Mróz and simply note that the resulting equations are identical. It is also observed that (13.12) fits into the framework (10.15).

With expression (13.7), we find that

$$\boxed{\sigma_{ij}^M - \sigma_{ij} = (a-1)(\sigma_{ij} - \alpha_{ij}^{(n)}) + \alpha_{ij}^{(n+1)} - \alpha_{ij}^{(n)}}$$

where all terms on the right-hand side are known quantities. Therefore, in the evolution law (13.12) it remains to identify the quantity q and we will return to this shortly. Before that we observe that if $\alpha_{ij}^{(n)} = \alpha_{ij}^{(n+1)}$ then $\sigma_{ij}^M - \sigma_{ij}$ becomes proportional to $\sigma_{ij} - \alpha_{ij}^{(n)}$, i.e. the evolution law (13.12) becomes similar to

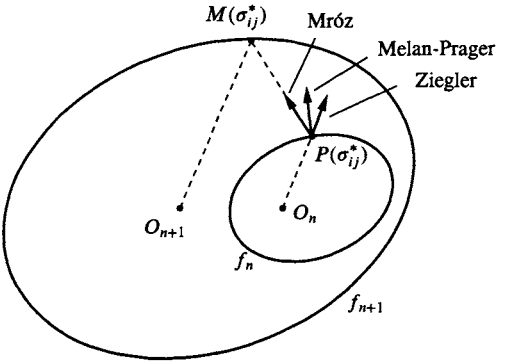

Figure 13.10: Comparison of different kinematic evolution laws; associated plasticity.

Ziegler's evolution law (12.82). In the general situation, however, the evolution laws of Melan-Prager, Ziegler and Mróz are compared in Fig. 13.10.

For clarity, let us recall that:

The largest yield surface that moves in the stress space is called the active yield surface and it is denoted by f_n

The non-associated flow rule reads

$$\dot{\varepsilon}_{ij}^p = \dot{\lambda}\frac{\partial g}{\partial \sigma_{ij}} \tag{13.13}$$

where g, as usual, denotes the potential function, which is equal to f_n for associated plasticity. Moreover, the consistency relation takes the form

$$\dot{f}_n = \frac{\partial f_n}{\partial \sigma_{ij}}\dot{\sigma}_{ij} + \frac{\partial f_n}{\partial \alpha_{ij}^{(n)}}\dot{\alpha}_{ij}^{(n)} = 0 \tag{13.14}$$

In view of (13.5), it follows that

$$\frac{\partial f_n}{\partial \sigma_{ij}} = \frac{\partial f_n}{\partial(\sigma_{kl} - \alpha_{kl}^{(n)})}\frac{\partial(\sigma_{kl} - \alpha_{kl}^{(n)})}{\partial \sigma_{ij}} = \frac{\partial f_n}{\partial(\sigma_{ij} - \alpha_{ij}^{(n)})}$$

$$\frac{\partial f_n}{\partial \alpha_{ij}^{(n)}} = \frac{\partial f_n}{\partial(\sigma_{kl} - \alpha_{kl}^{(n)})}\frac{\partial(\sigma_{kl} - \alpha_{kl}^{(n)})}{\partial \alpha_{ij}^{(n)}} = -\frac{\partial f_n}{\partial(\sigma_{ij} - \alpha_{ij}^{(n)})}$$

i.e.

$$\frac{\partial f_n}{\partial \alpha_{ij}^{(n)}} = -\frac{\partial f_n}{\partial \sigma_{ij}} \tag{13.15}$$

Insertion into (13.14) and use of (13.12) then give

$$\boxed{\frac{\partial f_n}{\partial \sigma_{ij}}\dot{\sigma}_{ij} - H_n\dot{\lambda} = 0} \tag{13.16}$$

where the plastic modulus H_n applicable between surface f_n and f_{n+1} is given by

$$H_n = q\frac{\partial f_n}{\partial \sigma_{ij}}(\sigma_{ij}^M - \sigma_{ij})$$

It appears that the quantity q present in the evolution law (13.12) is given by

$$\boxed{q = \frac{H_n}{\frac{\partial f_n}{\partial \sigma_{ij}}(\sigma_{ij}^M - \sigma_{ij})}} \tag{13.17}$$

As discussed previously, the fundamental concept of the Mróz model is the multilinear response; therefore, we have

$$\boxed{H_n = constant}$$

In the Mróz model, the plastic moduli H_n $(n = 0, 1, 2, \cdots)$ are chosen. For the active yield surface in question, (13.17) then determines the corresponding quantity q and the evolution law (13.12) is then identified completely. All fundamental equations in the Mróz model have then been established.

In relation to Fig. 13.7, it was observed that the stabilized cyclic stress-strain curve was obtained already after one cycle; this means that neither softening nor hardening effects are present. As discussed by Mróz (1967), the model described above may be generalized to consider such effects. Instead of (13.1), we now allow that the yield stresses σ_{yn} may vary, i.e. we have $\sigma_{yn} = \sigma_{yn}(\kappa)$, where κ is an internal variable. For instance, we may choose $\kappa = \lambda$, i.e.

$$\sigma_{yn} = \sigma_{yn}(\lambda) \; ; \quad n = 0, 1, 2, \cdots \tag{13.18}$$

The evolution law (13.12) is unchanged, but (13.5) and (13.18) now imply the following consistency relation

$$\dot{f}_n = \frac{\partial f_n}{\partial \sigma_{ij}}\dot{\sigma}_{ij} + \frac{\partial f_n}{\partial \alpha_{ij}^{(n)}}\dot{\alpha}_{ij}^{(n)} + \frac{\partial f_n}{\partial \lambda}\dot{\lambda} = 0 \tag{13.19}$$

where

$$\frac{\partial f_n}{\partial \lambda} = -p(\sigma_{yn})^{p-1}\frac{d\sigma_{yn}(\lambda)}{d\lambda}$$

With this expression and (13.12), (13.19) becomes

$$\frac{\partial f_n}{\partial \sigma_{ij}}\dot{\sigma}_{ij} - H_n\dot{\lambda} = 0$$

where the plastic modulus H_n is defined by

$$H_n = q\frac{\partial f_n}{\partial \sigma_{ij}}(\sigma_{ij}^M - \sigma_{ij}) + p(\sigma_{yn})^{p-1}\frac{d\sigma_{yn}(\lambda)}{d\lambda}$$

The quantity q is then defined by

$$q = \frac{H_n - p(\sigma_{yn})^{p-1}\frac{d\sigma_{yn}(\lambda)}{d\lambda}}{\frac{\partial f_n}{\partial \sigma_{ij}}(\sigma_{ij}^M - \sigma_{ij})} \tag{13.20}$$

In addition to the expression $\sigma_{yn} = \sigma_{yn}(\lambda)$, we choose as before a constant value for the plastic modulus H_n and (13.20) then determines the quantity q to be used in the evolution law (13.12).

13.1.1 von Mises yield function

Let us finally illustrate the pertinent equations for associated plasticity when a von Mises concept is adopted. For simplicity, the yield stresses σ_{yn} are taken as constants. The main thing that we want to discuss is the interpretation of the plastic modulus H_n. With (13.5) where $p = 1$ and F_n is given by (13.3), the flow rule (13.13) becomes

$$\dot{\varepsilon}_{ij}^p = \dot{\lambda}\frac{3(\sigma_{ij} - \alpha_{ij}^{d(n)})}{2\sigma_{yn}} \tag{13.21}$$

As usual, define the effective plastic strain rate by

$$\dot{\varepsilon}_{eff}^p = (\frac{2}{3}\dot{\varepsilon}_{ij}^p\dot{\varepsilon}_{ij}^p)^{1/2} \tag{13.22}$$

For uniaxial stressing, we have $\dot{\varepsilon}_{22}^p = \dot{\varepsilon}_{33}^p = -\dot{\varepsilon}_{11}^p/2$, i.e. $\dot{\varepsilon}_{eff}^p = |\dot{\varepsilon}_{11}^p|$, as usual. Moreover, insertion of (13.21) into (13.22) shows that

$$\dot{\varepsilon}_{eff}^p = \dot{\lambda}$$

Multiply the consistency relation (13.16) by $\dot{\lambda}$ and use the flow rule (13.13) for associated plasticity to obtain

$$\dot{\varepsilon}_{ij}^p\dot{\sigma}_{ij} = (\dot{\varepsilon}_{eff}^p)^2 H_n$$

For uniaxial stress conditions, the term $\dot{\varepsilon}_{ij}^p\dot{\sigma}_{ij}$ reduces to $\dot{\varepsilon}_{11}^p\dot{\sigma}_{11}$, i.e.

$$\frac{d\sigma_{11}}{d\varepsilon_{11}^p} = H_n$$

just like in the previous von Mises models.

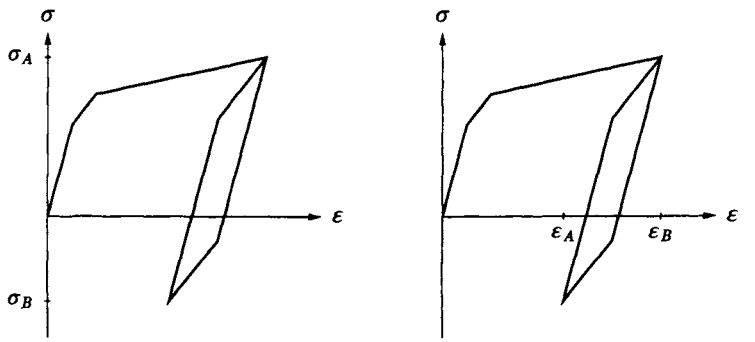

Figure 13.11: a) unsymmetrical stress cycling; b) unsymmetrical strain cycling.

It also readily follows that the elasto-plastic stiffness matrix $\boldsymbol{D}^{ep}$ is completely similar to that applicable to linear kinematic hardening, cf. (12.51).

For symmetric stress and strain cycles, the response has already been illustrated in Fig. 13.7. For cycling between unsymmetric stress states, the result in Fig. 13.11a) is obtained; no ratcheting is predicted and the stabilized cyclic stress-strain curve is already obtained after one cycle. Similarly, Fig. 13.11b) shows unsymmetrical strain cycling; no mean stress relaxation is predicted and the stabilized cyclic stress-strain curve is obtained after one cycle, and since it is symmetric, there is no difference between stress cycling and strain cycling. Despite these deficiencies, it is evident that the Mróz model is much better suited for cyclic loadings than the previously considered models. This is especially true if the multilinear approach contains many small segments such that a smooth curved response is approached. However, in a computer program this increases the storage requirements significantly, since each yield surface requires the storage of the six components of $\alpha_{ij}^{(n)}$ (as well as of σ_{yn} if this yield stress is allowed to vary).

13.2 Bounding surface models

In the Mróz model, the plastic modulus is constant in the region between two yield surfaces; this in turn leads to a multilinear response. We will now discuss an interesting formulation which makes use of only two yield surfaces and where the plastic modulus varies continuously between these two surfaces. This formulation forms the basis for many recent models and we will therefore provide a rather detailed discussion.

The concept we will discuss is the *bounding surface model* proposed simultaneously by Dafalias and Popov (1975, 1976) and Krieg (1975). Since the model of Dafalias and Popov was formulated in a more general manner, we will

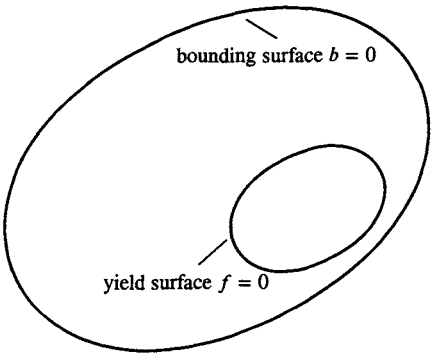

Figure 13.12: Yield surface and bounding surface in stress space.

here focus on this model.

The model contains two surfaces: a *bounding surface* and a *yield surface*, cf. Fig. 13.12. For evident reasons, the model is often called a *two-surface plasticity model*. During plastic loading, both the bounding surface and the yield surface may move and change size and they may come into contact with each other; however, the bounding surface always encloses the yield surface. The region inside the yield surface corresponds to an elastic response and plastic loading requires the current stress point to be located on the yield surface. The key issue is that it is the proximity of the two surfaces that determines the plastic modulus.

Let the yield surface f and the bounding surface b be defined by

$$\boxed{\begin{aligned} f &= F(\sigma_{ij} - \alpha_{ij}) - (\sigma_y)^p = 0 \quad \textit{yield surface} \\ b &= F(\sigma_{ij} - \beta_{ij}) - (\sigma_b)^p = 0 \quad \textit{bounding surface} \end{aligned}} \tag{13.23}$$

Here, the back-stress α_{ij} denotes the center of the yield surface whereas the back-stress β_{ij} denotes the center of the bounding surface. The parameters σ_y and σ_b, which have the dimensions of stress, depend in general on some internal variables κ_α, i.e.

$$\boxed{\sigma_y = \sigma_y(\kappa_\alpha) \;; \quad \sigma_b = \sigma_b(\kappa_\alpha)} \tag{13.24}$$

In order that the function F appearing in (13.23) possess the correct dimension, it is required that F be a homogeneous function of degree p in the variables $\sigma_{ij} - \alpha_{ij}$ (or $\sigma_{ij} - \beta_{ij}$). Referring to (13.6), this means that

$$\boxed{F(a(\sigma_{ij} - \alpha_{ij})) = a^p F(\sigma_{ij} - \alpha_{ij})} \tag{13.25}$$

where a is a quantity.

To determine the rules for how the back-stresses α_{ij} and β_{ij} change, we make use of the concepts introduced when the Mróz model was discussed. In the

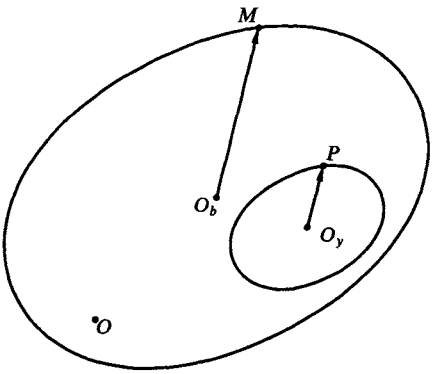

Figure 13.13: Current stress point P and mapping stress point M.

general stress space shown in Fig. 13.13, O denotes the origin of the stress space, O_y is the center of the yield surface and O_b is the center of the bounding surface. Assume that the current stress state σ_{ij} is located at point P on the yield surface. Define the mapping stress σ_{ij}^M located on the bounding surface at point M, where the point M is determined by the requirement that vector O_bM is parallel with vector O_yP. This means that

$$\boxed{\sigma_{ij}^M - \beta_{ij} = a(\sigma_{ij} - \alpha_{ij}) \; ; \quad a > 1} \tag{13.26}$$

where a is a proportionality factor. To determine this factor, we have from (13.23)

$$\frac{F(\sigma_{ij}^M - \beta_{ij})}{F(\sigma_{ij} - \alpha_{ij})} = (\frac{\sigma_b}{\sigma_y})^p \tag{13.27}$$

Moreover, (13.25) and (13.26) give

$$F(\sigma_{ij}^M - \beta_{ij}) = a^p F(\sigma_{ij} - \alpha_{ij})$$

Insertion into (13.27) provides

$$\boxed{a = \frac{\sigma_b}{\sigma_y}} \tag{13.28}$$

With this result, (13.26) determines the mapping stress σ_{ij}^M uniquely. From (13.26), we have

$$\boxed{\sigma_{ij}^M - \sigma_{ij} = (a-1)(\sigma_{ij} - \alpha_{ij}) + \beta_{ij} - \alpha_{ij}} \tag{13.29}$$

Similar to the discussion of the Mróz model, we conclude that the normals at point P and point M are parallel, cf. (13.11). Following again the discussion

of the Mróz model, it is required that the bounding surface and the yield surface never intersect and that contact occurs tangentially. This is achieved if the motion of the yield surface relative to the motion of the bounding surface occurs in the direction of vector PM, cf. Fig. 13.13. Therefore

$$\boxed{\dot{\alpha}_{ij} - \dot{\beta}_{ij} = \dot{\lambda}\, q^*(\sigma_{ij}^M - \sigma_{ij})} \tag{13.30}$$

where q^* is a positive quantity to be determined later. To be precise, Dafalias and Popov (1975, 1976) did not introduce the plastic multiplier $\dot{\lambda}$ at this point. However, in order to be consistent with the theoretical framework adopted here, we will deviate somewhat from the exposition of Dafalias and Popov and simply note that the resulting equations are identical.

The non-associated flow rule reads

$$\boxed{\dot{\varepsilon}_{ij}^p = \dot{\lambda}\frac{\partial g}{\partial \sigma_{ij}}} \tag{13.31}$$

where g, as usual, denotes the potential function, which is equal to f for associated plasticity. With (13.23) and (13.24), the consistency relation becomes

$$\dot{f} = \frac{\partial f}{\partial \sigma_{ij}}\dot{\sigma}_{ij} + \frac{\partial f}{\partial \alpha_{ij}}\dot{\alpha}_{ij} + \frac{\partial f}{\partial \kappa_\alpha}\dot{\kappa}_\alpha = 0$$

Similar to (13.15), we have $\partial f/\partial \alpha_{ij} = -\partial f/\partial \sigma_{ij} = -\partial F/\partial \sigma_{ij}$ and we then obtain

$$\frac{\partial F}{\partial \sigma_{ij}}\dot{\sigma}_{ij} - \frac{\partial F}{\partial \sigma_{ij}}\dot{\alpha}_{ij} - p(\sigma_y)^{p-1}\frac{\partial \sigma_y}{\partial \kappa_\alpha}\dot{\kappa}_\alpha = 0 \tag{13.32}$$

In order to proceed, we have, as usual, to specify the evolution laws for $\dot{\alpha}_{ij}$ and $\dot{\kappa}_\alpha$ and insert these expressions into the consistency relation (13.32). Most often, we have assumed that the evolution functions depend on the stresses σ_{ij} and the hardening parameters K_α, cf. (10.13). Referring to (13.23), we have two sets of hardening parameters for the yield criterion: one given by the back-stress α_{ij} and the other relating to the quantity σ_y. As usual, we may write $\sigma_y = \sigma_y(\kappa_\alpha)$ as

$$\boxed{\sigma_y = \sigma_{yo} + K(\kappa_\alpha)}$$

where σ_{yo} is some initial yield stress and K is the hardening parameter related to σ_y. In accordance with (10.13), we therefore take

$$\boxed{\dot{\kappa}_\alpha = \dot{\lambda} k_\alpha \quad \textit{where} \quad k_\alpha = k_\alpha(\sigma_{ij} - \alpha_{ij}, K(\kappa_\beta))} \tag{13.33}$$

For the evolution function relating to $\dot{\alpha}_{ij}$ and in accordance with the similar discussion following (10.13), we shall allow the following more general formulation

$$\boxed{\dot{\alpha}_{ij} = \dot{\lambda} q_{ij}^{(y)} \quad \textit{where} \quad q_{ij}^{(y)} = q_{ij}^{(y)}(\sigma_{ij} - \alpha_{ij}, K(\kappa_\beta), \delta, \delta_{in})} \tag{13.34}$$

where superscript (y) indicates that the back-stress α_{ij} is related to the yield surface. The variables δ and δ_{in} are so-called *discrete memory parameters*. The discrete memory parameter δ is defined as the distance between the mapping stress point σ_{ij}^M and the current stress point σ_{ij}, i.e.

$$\boxed{\delta = [(\sigma_{ij}^M - \sigma_{ij})(\sigma_{ij}^M - \sigma_{ij})]^{1/2}} \tag{13.35}$$

According to (13.29), the discrete memory parameter δ is known at every state during plastic loading. The discrete memory parameter δ_{in} is defined as δ at initiation of a plastic loading process:

$$\boxed{\delta_{in} = \textit{initial value of } \delta\textit{, i.e. the value of } \delta \textit{ every time a plastic loading process is initiated}}$$

For continued plastic loading, δ_{in} is kept constant, i.e. δ_{in} is only updated every time an elastic response is followed by plastic loading.

Whereas the definition of δ is unique, the definition of δ_{in} is more vague and, in fact, several possibilities exist. We will return later to a more specific definition of δ_{in} and it will turn out that a consistent definition of δ_{in} that works for general three-dimensional loading is not trivial; in fact, we will see that whereas the bounding surface model of Dafalias and Popov (1975, 1976) exhibits a number of appealing properties, the main drawback relates to a reasonable definition of δ_{in}.

Before we enter into a more detailed discussion of the definition of δ_{in}, we observe that δ is only defined during plastic loading whereas δ_{in} is constant during plastic loading and it is only updated when an elastic response is followed by plastic response. Therefore, both δ and δ_{in} may vary discontinuously and this is the reason for the term: *discrete memory parameters*; they memorize the load history and they do that in a discrete manner. We emphasize that δ and δ_{in} are not internal variables since internal variables only change during plastic loading, cf. (10.13). Considering, for instance, δ_{in} this quantity takes one constant value at initiation of plasticity; after elastic unloading and subsequent plastic reloading, δ_{in} takes another constant value. This means that δ_{in} is changed because of elastic unloading and, consequently, δ_{in} cannot be an internal variable.

After this discussion of the evolution laws for $\dot{\kappa}_\alpha$ and $\dot{\alpha}_{ij}$, we insert (13.33) and (13.34) into the consistency relation (13.32) to obtain

$$\boxed{\frac{\partial F}{\partial \sigma_{ij}}\dot{\sigma}_{ij} - H\dot{\lambda} = 0} \tag{13.36}$$

where the plastic modulus H is defined by

$$\boxed{H = H^{kin} + H^{iso}} \tag{13.37}$$

and where H^{kin} and H^{iso} are defined by

$$\boxed{H^{kin} = \frac{\partial F}{\partial \sigma_{ij}} q_{ij}^{(y)} \; ; \quad H^{iso} = p(\sigma_y)^{p-1} \frac{\partial \sigma_y}{\partial \kappa_\alpha} k_\alpha} \tag{13.38}$$

It appears that the plastic modulus has been split into two parts: one related to the kinematic hardening and another related to the isotropic hardening.

The fundamental issue of the bounding surface theory of Dafalias and Popov (1975, 1976) will now be introduced. It is assumed that the plastic modulus H depends on the current distance δ as well as on the initial distance δ_{in}:

$$\boxed{H = H(\delta, \delta_{in})} \tag{13.39}$$

Moreover, the plastic modulus H is specified by us, i.e. we choose the expression indicated by (13.39); we will later return to a suitable explicit expression. In (13.37), we also choose the quantity H^{iso}, i.e. how σ_y varies with the internal variables κ_α. Moreover, we also choose the direction of $\dot{\alpha}_{ij}$ that means the direction of $q_{ij}^{(y)}$. Having chosen H, H^{iso} and the direction of $q_{ij}^{(y)}$, (13.37) and (13.38) finally determine the magnitude of $q_{ij}^{(y)}$. We may summarize this discussion by

$$\boxed{\begin{minipage}{0.85\textwidth}*$H = H(\delta, \delta_{in})$ and H^{iso} are chosen by us. Also the direction of $q_{ij}^{(y)}$ is specified by us. Expressions (13.37) and (13.38) then determine the magnitude of $q_{ij}^{(y)}$. In turn, the evolution law for $\dot{\alpha}_{ij}$ has then been determined completely.*\end{minipage}} \tag{13.40}$$

It is of interest that this format allows any kinematic hardening rule to be chosen for $\dot{\alpha}_{ij}$. For instance, we may choose the direction of $\dot{\alpha}_{ij}$ according to Melan-Prager's, Ziegler's or Mróz's evolution laws, to which we will later return.

When the yield surface and the bounding surface are in contact with each other, $\delta = 0$ holds. The corresponding value of H turns out to be of particular interest and we use the following notation:

$$\boxed{H_o = H(\delta = 0, \delta_{in})} \tag{13.41}$$

This means that the plastic modulus applicable when the yield surface and bounding surface are in contact is the plastic modulus H_o.

According to the discussion relating to (13.40), any kinematic hardening rule can be chosen for the direction of $\dot{\alpha}_{ij}$. In general, however, the bounding surface also moves in the stress space and (13.30) relates the back-stress rates $\dot{\alpha}_{ij}$ to $\dot{\beta}_{ij}$ via the unspecified quantity q^*. Let us therefore determine this quantity.

Similar to (13.34), the evolution law for $\dot{\beta}_{ij}$ can be written in the following general format

$$\dot{\beta}_{ij} = \dot{\lambda} q_{ij}^{(b)} \tag{13.42}$$

where superscript (b) indicates that the back-stress β_{ij} is related to the bounding surface. Multiplication of (13.30) by $\partial F/\partial\sigma_{ij}$ and use of the evolution laws (13.34) and (13.42) then lead to

$$\frac{\partial F}{\partial\sigma_{ij}}q_{ij}^{(y)} - \frac{\partial F}{\partial\sigma_{ij}}q_{ij}^{(b)} = q^*\frac{\partial F}{\partial\sigma_{ij}}(\sigma_{ij}^M - \sigma_{ij}) \tag{13.43}$$

Let us define the quantity $\tilde{H}$ by

$$\tilde{H} = \frac{\partial F}{\partial\sigma_{ij}}q_{ij}^{(b)} \tag{13.44}$$

With (13.38), (13.43) then gives

$$q^* = \frac{H^{kin} - \tilde{H}}{\frac{\partial F}{\partial\sigma_{ij}}(\sigma_{ij}^M - \sigma_{ij})} \tag{13.45}$$

It appears that q^* is known once the quantity $\tilde{H}$ is known. Let us now make the assumption that $\tilde{H}$ only depends on the initial distance δ_{in} as well as on the internal variables κ_α, i.e.

$$\tilde{H} = \tilde{H}(\delta_{in}, \kappa_\alpha) \tag{13.46}$$

To determine $\tilde{H}$, we apply that the mapping stress σ_{ij}^M is located on the bounding surface, i.e. (13.23) gives $b = F(\sigma_{ij}^M - \beta_{ij}) - (\sigma_b)^p = 0$. Since σ_{ij}^M is always located on the bounding surface, the consistency relation $\dot{b} = 0$ for the bounding surface then reads

$$\frac{\partial F(\sigma_{kl}^M - \beta_{kl})}{\partial\sigma_{ij}^M}\dot{\sigma}_{ij}^M + \frac{\partial F(\sigma_{kl}^M - \beta_{kl})}{\partial\beta_{ij}}\dot{\beta}_{ij} - p(\sigma_b)^{p-1}\frac{\partial\sigma_b}{\partial\kappa_\alpha}\dot{\kappa}_\alpha = 0$$

As usual, cf. (13.15), we have $\partial F(\sigma_{kl}^M - \beta_{kl})/\partial\beta_{ij} = -\partial F(\sigma_{kl}^M - \beta_{kl})/\partial\sigma_{ij}^M$, which with (13.33) leads to

$$\frac{\partial F(\sigma_{kl}^M - \beta_{kl})}{\partial\sigma_{ij}^M}\dot{\sigma}_{ij}^M - \frac{\partial F(\sigma_{kl}^M - \beta_{kl})}{\partial\sigma_{ij}^M}\dot{\beta}_{ij} - p(\sigma_b)^{p-1}\frac{\partial\sigma_b}{\partial\kappa_\alpha}k_\alpha\dot{\lambda} = 0 \tag{13.47}$$

Moreover, similar to (13.11) we have

$$\frac{\partial F(\sigma_{kl}^M - \beta_{kl})}{\partial\sigma_{ij}^M} = a^{p-1}\frac{\partial F(\sigma_{kl} - \beta_{kl})}{\partial\sigma_{ij}} = a^{p-1}\frac{\partial F}{\partial\sigma_{ij}}$$

i.e. (13.47) takes the form

$$a^{p-1}\frac{\partial F}{\partial\sigma_{ij}}\dot{\sigma}_{ij}^M - a^{p-1}\tilde{H}\dot{\lambda} - p(\sigma_b)^{p-1}\frac{\partial\sigma_b}{\partial\kappa_\alpha}k_\alpha\dot{\lambda} = 0 \tag{13.48}$$

where advantage also was taken of (13.42) and (13.44). The expression above holds in general and it therefore also holds for the special case of contact between the yield surface and the bounding surface. On contact, we have $\dot{\sigma}_{ij}^M = \dot{\sigma}_{ij}$, i.e. $\partial F/\partial\sigma_{ij}\dot{\sigma}_{ij}^M = \partial F/\partial\sigma_{ij}\dot{\sigma}_{ij} = H\dot{\lambda}$ where (13.36) was used. On contact, the current distance $\delta = 0$ and the plastic modulus H then takes the value H_o, cf. (13.41). With these remarks and noting that $\tilde{H}$ is independent of the current distance δ, cf. (13.46), evaluation of (13.48) on contact leads to

$$\tilde{H} = H_o - p(\sigma_y)^{p-1}\frac{\partial\sigma_b}{\partial\kappa_\alpha}k_\alpha \tag{13.49}$$

where (13.28) was used. All terms on the right-hand side are known quantities that determine $\tilde{H}$ uniquely. Insertion of (13.49) into (13.45) and use of (13.37) then provide

$$\boxed{q^* = \frac{H - H_o - H^{iso} + p(\sigma_y)^{p-1}\frac{\partial\sigma_b}{\partial\kappa_\alpha}k_\alpha}{\frac{\partial F}{\partial\sigma_{ij}}(\sigma_{ij}^M - \sigma_{ij})}} \tag{13.50}$$

Once the quantity q^* has been determined, the evolution of $\dot{\beta}_{ij}$ is given by (13.30), i.e.

$$\boxed{\dot{\beta}_{ij} = \dot{\alpha}_{ij} - \dot{\lambda}\, q^*(\sigma_{ij}^M - \sigma_{ij})} \tag{13.51}$$

All quantities of interest in the Dafalias-Popov model have then been identified.

If neither the yield surface nor the bounding surface experience isotropic hardening, then the numerator of the expression for q^* reduces to $H - H_o$, which becomes zero on contact; during contact, we therefore have $\dot{\beta}_{ij} = \dot{\alpha}_{ij}$, as expected. However, if isotropic hardening is involved, we have $\dot{\beta}_{ij} \neq \dot{\alpha}_{ij}$ even during contact.

Let us return to the expression for the plastic modulus H given in general by (13.39). The explicit form of this expression is specified by us and, evidently, many choices are possible. A particularly simple and advantageous form was suggested by Dafalias and Popov (1976) and it reads

$$\boxed{H(\delta, \delta_{in}) = H_o + \frac{\delta}{\delta_{in} - \delta}h} \tag{13.52}$$

where both H_o and the positive parameter h are taken as constants. On contact, this expression provides $H = H_o$ as required; moreover, at every event where plastic loading is initiated, we have $\delta_{in} = \delta$, i.e. $H \to \infty$. This implies a smooth transition when going from an elastic to a plastic response and, as discussed later, this property is often very close to experimental evidence.

13.2.1 von Mises yield function

Let us below illustrate the Dafalias-Popov model for associated plasticity within a von Mises concept. Only kinematic hardening will be considered and (13.23) then reduces to

$$\begin{aligned} f &= [\tfrac{3}{2}(s_{ij} - \alpha^d_{ij})(s_{ij} - \alpha^d_{ij})]^{1/2} - \sigma_{yo} = 0 \\ b &= [\tfrac{3}{2}(s_{ij} - \beta^d_{ij})(s_{ij} - \beta^d_{ij})]^{1/2} - \sigma_{bo} = 0 \end{aligned} \tag{13.53}$$

where σ_{yo} and σ_{bo} are taken as constant quantities whereas α^d_{ij} and β^d_{ij}, as usual, denote the deviatoric parts of the back-stresses. The flow rule (13.31) then becomes

$$\dot{\varepsilon}^p_{ij} = \dot{\lambda}\frac{3(s_{ij} - \alpha^d_{ij})}{2\sigma_{yo}} \tag{13.54}$$

As usual, we have

$$\dot{\lambda} = \dot{\varepsilon}^p_{eff} \quad \text{where} \quad \dot{\varepsilon}^p_{eff} = (\frac{2}{3}\dot{\varepsilon}^p_{ij}\dot{\varepsilon}^p_{ij})^{1/2} \tag{13.55}$$

Since only kinematic hardening is considered, (13.37) gives

$$H^{kin} = H \tag{13.56}$$

Moreover, (13.50) gives

$$q^* = \frac{2\sigma_{yo}(H - H_o)}{3(s_{ij} - \alpha^d_{ij})(s^M_{ij} - s_{ij})} \tag{13.57}$$

In general, δ is the distance between the mapping stress point σ^M_{ij} and the current stress point σ_{ij}, cf. (13.35). However, since the plastic response of a von Mises material is assumed to depend on deviatoric quantities, only, δ is redefined according to

$$\delta = [(s^M_{ij} - s_{ij})(s^M_{ij} - s_{ij})]^{1/2} \tag{13.58}$$

Melan-Prager's evolution law

Assume that Melan-Prager's evolution law (12.80) holds for the back-stress α_{ij}, i.e.

$$\dot{\alpha}_{ij} = c\,\dot{\varepsilon}^p_{ij}$$

With (13.54) and (13.34), we find that

$$\dot{\alpha}_{ij} = \dot{\alpha}^d_{ij} = \dot{\lambda}c\frac{3(s_{ij} - \alpha^d_{ij})}{2\sigma_{yo}} \qquad \text{i.e.} \qquad q^{(y)}_{ij} = c\frac{3(s_{ij} - \alpha^d_{ij})}{2\sigma_{yo}} \tag{13.59}$$

From (13.38) and (13.56) it is then concluded that

$$c = \frac{2}{3}H \tag{13.60}$$

The evolution law for $\dot{\beta}_{ij}$ is given by (13.51). According to (13.53) it is only the deviatoric part $\dot{\beta}^d_{ij}$ that is of interest. Therefore, use of (13.59), (13.60) and (13.57) in (13.51) give

$$\dot{\beta}^d_{ij} = \dot{\lambda}\frac{H}{\sigma_{yo}}(s_{ij} - \alpha^d_{ij}) - \dot{\lambda}\frac{2\sigma_{yo}(H - H_o)}{3(s_{kl} - \alpha^d_{kl})(s^M_{kl} - s_{kl})}(s^M_{ij} - s_{ij}) \tag{13.61}$$

Ziegler's evolution law

Assume next that Ziegler's evolution law (12.82) holds for the back-stress α_{ij}. Adopting the formulation given by (12.84), we then have

$$\dot{\alpha}_{ij} = \dot{\lambda}k(\sigma_{ij} - \alpha_{ij}) \qquad \text{i.e.} \qquad q^{(y)}_{ij} = k(\sigma_{ij} - \alpha_{ij})$$

From (13.38) and (13.56) follow that

$$k = \frac{H}{\sigma_{yo}}$$

i.e.

$$\alpha^d_{ij} = \dot{\lambda}\frac{H}{\sigma_{yo}}(s_{ij} - \alpha^d_{ij})$$

Comparing with (13.59) and observing (13.60), it appears that we are back to the Melan-Prager formulation; this is certainly to be expected, cf. (12.87).

Mróz' evolution law

Finally, assume that Mróz' evolution law (13.12) holds for the back-stress α_{ij}, i.e.

$$\dot{\alpha}_{ij} = \dot{\lambda}\, q(\sigma^M_{ij} - \sigma_{ij}) \qquad \text{i.e.} \qquad q^{(y)}_{ij} = q(\sigma^M_{ij} - \sigma_{ij}) \tag{13.62}$$

With (13.38) and (13.56), we then obtain

$$q = \frac{2\sigma_{yo}H}{3(s_{ij} - \alpha^d_{ij})(s^M_{ij} - s_{ij})}$$

With (13.62) as well as (13.57), the evolution law (13.51) for $\dot{\beta}_{ij}$ then gives

$$\dot{\beta}_{ij} = \dot{\lambda}\frac{2\sigma_{yo}H_o}{3(s_{kl} - \alpha^d_{kl})(s^M_{kl} - s_{kl})}(\sigma^M_{ij} - \sigma_{ij}) \tag{13.63}$$

It may be observed that both (13.61) and (13.63) imply

$$\frac{\partial F}{\partial \sigma_{ij}}\dot{\beta}_{ij} = \frac{3(s_{ij} - \alpha^d_{ij})}{2\sigma_{yo}}\dot{\beta}^d_{ij} = \dot{\lambda}H_o \tag{13.64}$$

in accordance with (13.44) and (13.49).

13.2.2 Uniaxial loading

Let us finally specialize to purely uniaxial loading. In that case, we have

$$[\sigma_{ij}] = \begin{bmatrix} \sigma & 0 & 0 \\ 0 & 0 & 0 \\ 0 & 0 & 0 \end{bmatrix} \tag{13.65}$$

For uniaxial stressing, the most direct interpretation of the foregoing von Mises formulations turns out to be provided by Mróz' evolution law. Initially, before any plasticity is involved, we have $\alpha_{ij} = \beta_{ij} = 0$ and (13.26) then shows that, initially, σ_{ij}^M is proportional to σ_{ij}. From (13.62) and (13.63) then follow that both $\dot{\alpha}_{ij}$ and $\dot{\beta}_{ij}$ are initially proportional to σ_{ij}. This allows us to conclude that σ_{ij}^M, α_{ij} and β_{ij} are always proportional to σ_{ij}, i.e.

$$[\sigma_{ij}^M] = \begin{bmatrix} \sigma^M & 0 & 0 \\ 0 & 0 & 0 \\ 0 & 0 & 0 \end{bmatrix} ; \quad [\alpha_{ij}] = \begin{bmatrix} \alpha & 0 & 0 \\ 0 & 0 & 0 \\ 0 & 0 & 0 \end{bmatrix} ; \quad [\beta_{ij}] = \begin{bmatrix} \beta & 0 & 0 \\ 0 & 0 & 0 \\ 0 & 0 & 0 \end{bmatrix} \tag{13.66}$$

Insertion of (13.65) and (13.66b) into the yield criterion (13.53) gives

$$\sigma - \alpha = z\sigma_{yo} \tag{13.67}$$

where

$$\boxed{z = \begin{cases} 1 & \textit{for increasing stress} \\ -1 & \textit{for decreasing stress} \end{cases}}$$

Likewise, insertion of (13.66a) and (13.66c) into the bounding criterion (13.53) gives

$$\sigma^M - \beta = z\sigma_{bo} \tag{13.68}$$

The distance δ is defined by (13.58), which with (13.65) and (13.66a) becomes

$$\boxed{\delta = z\sqrt{\frac{2}{3}}(\sigma^M - \sigma)}$$

Let us finally determine the evolution expressions. For uniaxial conditions (13.55) shows that

$$\dot{\lambda} = z\dot{\varepsilon}^p \tag{13.69}$$

where $\dot{\varepsilon}^p = \dot{\varepsilon}_{11}^p$. Multiplication of the consistency relation (13.36) by $\dot{\lambda}$ and use of the associated flow rule result in

$$\dot{\varepsilon}_{ij}^p \dot{\sigma}_{ij} - (\dot{\lambda})^2 H = 0$$

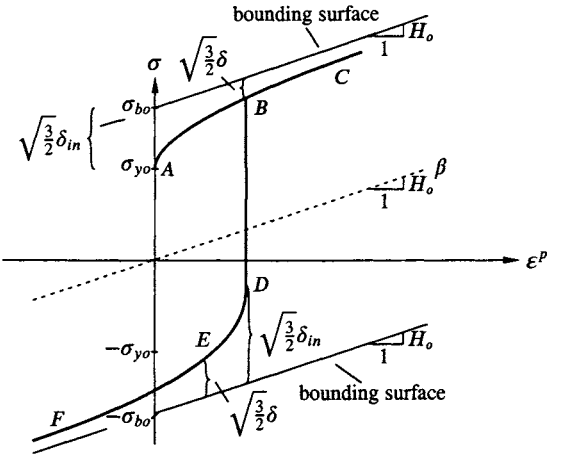

Figure 13.14: Bounding surface model.

For uniaxial conditions, this expression reduces to

$$\boxed{\dot{\sigma} = H\dot{\varepsilon}^p}$$

where the plastic modulus is given by (13.52). Expression (13.67) then shows that

$$\boxed{\dot{\alpha} = H\dot{\varepsilon}^p}$$

To determine how σ^M and β evolute with the loading, we first observe (13.65) and (13.66b) and find that

$$\frac{3(s_{ij} - \alpha_{ij}^d)}{2\sigma_{yo}}\dot{\beta}_{ij}^d = \frac{\sigma - \alpha}{\sigma_{yo}}\dot{\beta}$$

Insertion of this expression into (13.64) and taking advantage of (13.67) and (13.69) give

$$\boxed{\dot{\beta} = H_o\dot{\varepsilon}^p}$$

which with (13.68) leads to

$$\boxed{\dot{\sigma}^M = H_o\dot{\varepsilon}^p}$$

For uniaxial loading the response is shown in Fig. 13.14. For steadily increasing loading, the uniaxial curve will be described by ABC. If loading is reversed at point B, an elastic unloading will take place from B to D. At point D plastic reloading will start and the discrete memory parameter δ_{in} will be updated to the new distance. The plastic reloading will then follow DEF and this

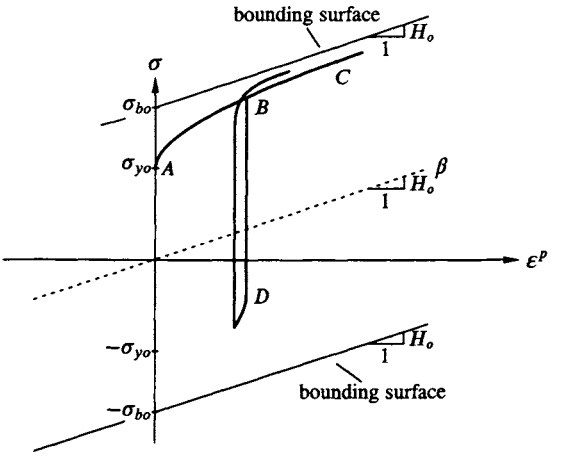

Figure 13.15: Illustration of overshooting effect.

response is in close agreement with the behavior of metals and steel; in particular the smooth transition, i.e. $H \to \infty$, when going from an elastic to a plastic response is attractive.

However, there exist some difficulties to be solved in this model. Assume, for instance, that we follow the path ABD and just touch the yield surface at point D such that the discrete memory parameter δ_{in} will be updated. Let the loading then be reversed once more. As a result δ_{in} will be updated at point B where we will have $\delta = \delta_{in}$, i.e. $H \to \infty$ implying that the stress-strain curve will be significantly above the curve BC, cf. 13.15. This so-called *overshooting* effect is clearly not acceptable and it is probably the largest deficiency in the bounding surface model.

13.3 Armstrong and Frederick model

As the last example let us consider a model introduced by Armstrong and Frederick (1966). This model has significant benefits as will be shown and it solves many of the problems relating to nonlinear kinematic hardening. The kinematic hardening model described here has been enhanced in various ways by many researchers to predict more and more complex material behavior.

For purely kinematic hardening, Armstrong and Frederick (1966) proposed the following evolution law for the back-stress tensor

$$\boxed{\dot{\alpha}_{ij} = h\left(\frac{2}{3}\dot{\varepsilon}^p_{ij} - \frac{\alpha_{ij}}{\alpha_\infty}\dot{\varepsilon}^p_{eff}\right); \quad \textit{Armstrong-Frederick evolution law}} \tag{13.70}$$

where h and α_∞ are constants, $\dot{\varepsilon}^p_{eff}$ is the effective plastic strain rate and α_{ij} is

the back-stress tensor defining the center of the yield surface. We note that by letting $\alpha_\infty \to \infty$, Melan-Prager's classical kinematic hardening law (12.46) is recovered. As will be shown later, the last term in (13.70) serves as a *recall term.*

It is of interest to consider purely isotropic hardening in a format similar to (13.70) and we take

$$\dot{K} = h(1 - \frac{K}{K_\infty})\dot{\varepsilon}^p_{eff} \tag{13.71}$$

where K measures the increase of the yield surface and h and K_∞ are constants. If $K_\infty \to \infty$, we obtain linear hardening with the plastic modulus h. Integration of (13.71) with $K(\varepsilon^p_{eff} = 0) = 0$ gives

$$K = K_\infty(1 - e^{-\frac{h\varepsilon^p_{eff}}{K_\infty}}) \tag{13.72}$$

i.e. exponential hardening with the asymptotic value K_∞, cf. (9.3); it also appears that strain hardening is used to model the isotropic hardening of the yield surface. For isotropic hardening von Mises plasticity given by (12.4), the maximum value of the yield stress will then become $\sigma_{yo} + K_\infty$, where σ_{yo} is the initial yield stress. From (13.72) we can draw the conclusion that the term h/α_∞ in (13.70) serves as a damping factor that determines how fast α_{ij} should approach its asymptotic value.

13.3.1 von Mises yield function

For a von Mises material, we will illustrate mixed hardening in terms of a combination of the Armstrong-Frederick kinematic hardening model with isotropic hardening and the great potential of the Armstrong-Frederick model will then become evident. The yield function can be written as

$$f = \bar{\sigma}_{eff} - \sigma_{yo} - K \tag{13.73}$$

where

$$\bar{\sigma}_{eff} = \left(\frac{3}{2}\bar{s}_{ij}\bar{s}_{ij}\right)^{1/2} ; \qquad \bar{s}_{ij} = s_{ij} - \alpha^d_{ij}$$

where $\bar{s}_{ij}$ is the reduced deviatoric stress tensor.

The flow rule provides

$$\dot{\varepsilon}^p_{ij} = \dot{\lambda}\frac{\partial f}{\partial \sigma_{ij}} = \dot{\lambda}\frac{3}{2}\frac{\bar{s}_{ij}}{\bar{\sigma}_{eff}} \tag{13.74}$$

and we have $\dot{\varepsilon}^p_{ii} = 0$, i.e. plastic incompressibility, as expected. The effective plastic strain rate is as usual defined as

$$\dot{\varepsilon}^p_{eff} = \left(\frac{2}{3}\dot{\varepsilon}^p_{ij}\dot{\varepsilon}^p_{ij}\right)^{1/2}$$

and making use of the flow rule (13.74), it then follows that

$$\boxed{\dot{\varepsilon}^p_{eff} = \dot{\lambda}} \tag{13.75}$$

This means that we can interpret the plastic multiplier $\dot{\lambda}$ in (13.74) as the rate of the effective plastic strain.

To obtain mixed hardening with the isotropic hardening described by (13.71) and the kinematic hardening described by (13.70) we adopt

$$\boxed{\begin{aligned} \dot{K} &= m\,h\left(1 - \frac{K}{K_\infty}\right)\dot{\varepsilon}^p_{eff} \\ \dot{\alpha}_{ij} &= (1-m)h\left(\frac{2}{3}\dot{\varepsilon}^p_{ij} - \frac{\alpha_{ij}}{\alpha_\infty}\dot{\varepsilon}^p_{eff}\right) \end{aligned}} \tag{13.76}$$

In fact, (13.76a) and (13.76b) are similar to the expressions adopted when Melan-Prager's linear kinematic hardening rule was used to derive a mixed isotropic/kinematic von Mises model cf. (12.65). It appears that for $m = 1$ a purely isotropic hardening model is obtained and for $m = 0$ a purely Armstrong-Frederick kinematic hardening model is obtained, and for values in between, a mixed formulation emerges

Since $\dot{\varepsilon}^p_{ij}$ is deviatoric and as $\alpha_{ij} = 0$ holds initially before plasticity is introduced, it follows that the back-stress α_{ij} will always be purely deviatoric, i.e.

$$\alpha_{ij} = \alpha^d_{ij}$$

It is also observed that the evolution laws (13.76) can be written in the general format given by (10.15).

To determine the response of the above model, we start by calculating an expression for the plastic modulus. Making use of the consistency relation, $\dot{f} = 0$, written in the standard form (10.16), we have

$$\frac{\partial f}{\partial \sigma_{ij}}\dot{\sigma}_{ij} - H\dot{\lambda} = 0 \tag{13.77}$$

where H is the plastic modulus. From (13.73), the consistency relation $\dot{f} = 0$ becomes

$$\dot{f} = \frac{\partial f}{\partial \sigma_{ij}}\dot{\sigma}_{ij} + \frac{\partial f}{\partial \alpha_{ij}}\dot{\alpha}_{ij} + \frac{\partial f}{\partial K}\dot{K} = 0$$

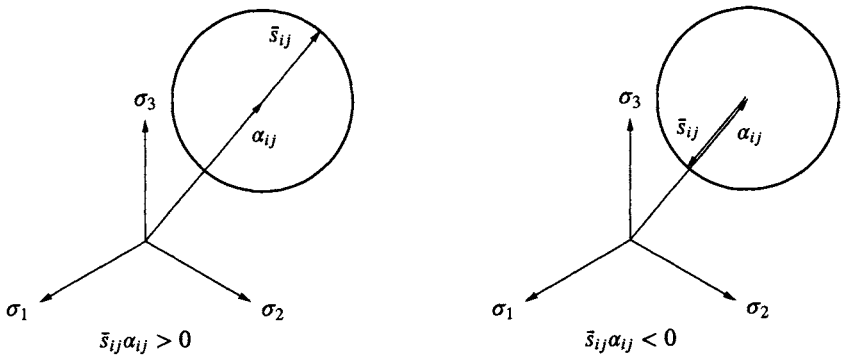

Figure 13.16: Illustration that the term $\bar{s}_{ij}\alpha_{ij}$ changes when the loading is reversed

Insertion of (13.76) as well as (13.74) and (13.75) and comparison with (13.77) then provide

$$H = -\frac{\partial f}{\partial \alpha_{ij}}(1-m)h(\frac{\bar{s}_{ij}}{\bar{\sigma}_{eff}} - \frac{\alpha_{ij}}{a_\infty}) - \frac{\partial f}{\partial K} mh(1 - \frac{K}{K_\infty})$$

Determination of $\partial f/\partial \alpha_{ij}$ and $\partial f/\partial K$ and use of the yield condition then leads to

$$H = h\left[(1-m)\left(1 - \frac{3}{2}\frac{\bar{s}_{ij}\alpha_{ij}}{\bar{\sigma}_{eff}\alpha_\infty}\right) + m\left(1 - \frac{K}{K_\infty}\right)\right] \tag{13.78}$$

The interesting part of the plastic modulus is the term $\bar{s}_{ij}\alpha^d_{ij}$, which obviously can change sign, depending upon the loading direction, i.e. the plastic modulus will change (increase) when the loading is reversed. This is the key property of the Armstrong-Frederick model and is illustrated in Fig. 13.16. It also appears that this property is due to the *recall* term $\alpha_{ij}/\alpha_\infty\ \dot{\varepsilon}^p_{ij}$ present in (13.70); this term 'recalls' –i.e. recovers– and thereby increases the plastic modulus when the loading is reversed.

To obtain an interpretation of the plastic modulus H, we multiply (13.77) by the plastic multiplier $\dot{\lambda}$ and use the flow rule as well as(13.75) to obtain

$$\dot{\varepsilon}^p_{ij}\dot{\sigma}_{ij} = H(\dot{\varepsilon}^p_{eff})^2$$

For uniaxial conditions, the term $\dot{\varepsilon}^p_{ij}\dot{\sigma}_{ij}$ reduces to $\dot{\varepsilon}^p_{11}\dot{\sigma}_{11}$ and we then obtain

$$\frac{d\sigma_{11}}{d\varepsilon^p_{11}} = H$$

as in other von Mises models.

To analyze the model in more detail, a monotonic proportional loading situation is considered and we will determine the relation between σ_{eff} and ε^p_{eff}. We have

$$s_{ij} = p(t)s^*_{ij} \tag{13.79}$$

where s^*_{ij} is an arbitrarily fixed deviatoric stress tensor, whereas $p(t)$ serves as the loading function. Before any plasticity is involved $\alpha_{ij} = 0$ holds, i.e. (13.76) and (13.74) imply that $\dot{\alpha}_{ij}$ initially is proportional to s_{ij} and thereby to s^*_{ij}. It follows that α_{ij} will be proportional to s^*_{ij} for proportional loading, i.e.

$$\alpha_{ij} = q(t)s^*_{ij} \tag{13.80}$$

Obviously, $q(t)$ and $p(t)$ are not independent loading functions. We can take $p(t)$ and $q(t)$ as positive functions and it is evident that $p(t) \geq q(t)$. With (13.79) and (13.80) it follows that

$$\bar{s}_{ij} = (p-q)s^*_{ij}\ ; \quad \bar{\sigma}_{eff} = (p-q)\sigma^*_{ij}\ ; \quad \sigma_{eff} = p\sigma^*_{eff} \tag{13.81}$$

Integration of (13.76a) with the initial condition that $K(\varepsilon^p_{eff} = 0) = 0$ gives

$$K = K_\infty(1 - e^{-\frac{mh}{K_\infty}\varepsilon^p_{eff}}) \tag{13.82}$$

For proportional loading, the flow rule (13.74) results in

$$\dot{\varepsilon}^p_{kl} = \dot{\varepsilon}^p_{eff}\frac{3}{2\sigma^*_{eff}}s^*_{kl}$$

Insertion into the evolution equation (13.76b) gives

$$\dot{q}s^*_{ij} = (1-m)h(\frac{1}{\sigma^*_{eff}} - \frac{q}{\alpha_\infty})\dot{\varepsilon}^p_{eff}s^*_{ij}$$

from which it is concluded that

$$\dot{q}\sigma^*_{eff} = (1-m)h(1 - \frac{q\sigma^*_{eff}}{\alpha_\infty})\dot{\varepsilon}^p_{eff}$$

With the initial condition $\varepsilon^p_{eff} = 0$ implies $q = 0$, integration of this differential equation in q gives

$$q\sigma^*_{eff} = \alpha_\infty(1 - e^{-\frac{(1-m)h}{\alpha_\infty}\varepsilon^p_{eff}}) \tag{13.83}$$

For proportional loading, the yield condition (13.73) is written as

$$(p-q)\sigma^*_{eff} - \sigma_{yo} - K = 0$$

which with (13.81c) becomes

$$\sigma_{eff} = p\sigma^*_{eff} = q\sigma^*_{eff} + \sigma_{yo} + K$$

Insertion of (13.82) and (13.83) results in

$$\sigma_{eff} = \sigma_{yo} + \alpha_\infty(1 - e^{-\frac{(1-m)h}{\alpha_\infty}\varepsilon^p_{eff}}) + K_\infty(1 - e^{-\frac{mh}{K_\infty}\varepsilon^p_{eff}}) \tag{13.84}$$

It appears that when $\varepsilon^p_{eff} \to \infty$ then $\sigma_{eff} \to \sigma_{yo} + \alpha_\infty + K_\infty$.

We want a mixed formulation such that for increasing proportional loading, the response is the same irrespective of the m-value. This is achieved by setting

$$\alpha_\infty + K_\infty = \text{constant} \tag{13.85}$$

Moreover, it is required that

$$\frac{1-m}{\alpha_\infty} = \frac{m}{K_\infty} \quad \Rightarrow \quad \frac{m}{K_\infty} = \frac{1}{\alpha_\infty + K_\infty} \tag{13.86}$$

and (13.84) then reduces to the result sought

$$\sigma_{eff} = \sigma_{yo} + (\alpha_\infty + K_\infty)(1 - e^{-\frac{h}{\alpha_\infty + K_\infty}\varepsilon^p_{eff}})$$

It then follows that

$$\frac{d\sigma_{eff}}{d\varepsilon^p_{eff}} = he^{-\frac{h}{\alpha_\infty + K_\infty}\varepsilon^p_{eff}}$$

and the initial slope for $\varepsilon^p_{eff} = 0$ is given by h.

The prediction of the model in uniaxial loading is illustrated in Figs. 13.17-13.20. In these examples we have used the constraints given by (13.85) and (13.86) such that the initial loading curves are the same irrespective of the m-value. From Fig. 13.17 it appears that the model is capable of predicting a realistic nonlinear response both during loading and reversal loading. The figure also shows the interpretation of the asymptotic value $\sigma_{yo} + \alpha_\infty + K_\infty$, as well as the interpretation of H and h. It appears that by a proper choice of material parameter m, we can simulate a response that is in much closer agreement with reality than the mixed hardening von Mises model with linear hardening, cf. Fig 12.21.

The response during symmetrical loading conditions is shown in Fig. 13.18, for $m = 0$; it shows that the response of the model stabilizes after one cycle. Introducing also isotropic hardening into the model gives the response shown in Fig 13.19; due to the increase of the elastic region the response stabilizes after some cycles. Note that in the cyclic stabilized state we have that $K = K_\infty$, i.e. no additional isotropic hardening occurs. Therefore considering the symmetric

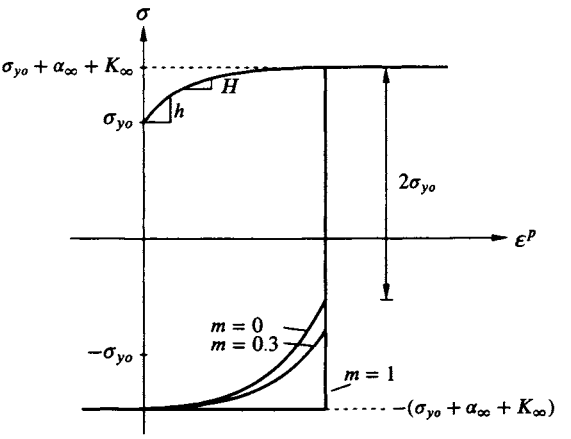

Figure 13.17: Prediction of mixed hardening von Mises model with Armstrong-Frederick's hardening rule

stress cycling case, increase of the stress amplitude after a stabilized state has been achieved will give a response where we only have kinematic hardening, and for subsequent cyclic loading the stabilized cycle is then obtained after one cycle, just like in Fig. 13.18.

To show some deficiencies of the model, we choose $m = 0$, i.e. the purely kinematic hardening case, and the responses for unsymmetric cycling are then shown in Fig. 13.20. For unsymmetric strain cycling, the model shows the desired property that the mean stress relaxes to zero, but as indicated in Fig. 13.20a it takes place within a very few cycles. Referring to Fig. 13.20b, this property of the model is more clearly evident if unsymmetric stress cycling is considered, where the model will show a very large ratcheting behavior with a constant $\Delta\varepsilon^p$-value in every cycle. For a stable material, one should expect a decreasing ratcheting behavior with $\Delta\varepsilon^p \to 0$ as the unsymmetric stress cycling is continued.

It might be in order to say something about the development and improvement of the Armstrong-Frederick model. A generalization introduced by Chaboche *et al.* (1979) and Chaboche (1989); Chaboche (1989) is based on superposition of several nonlinear kinematic hardening rules according to

$$\alpha_{ij} = \sum_{n=1}^{m} \alpha_{ij}^n \tag{13.87}$$

$$\dot{\alpha}_{ij}^n = h^n \left(\frac{2}{3}\dot{\varepsilon}_{ij}^p - \frac{\alpha_{ij}^n}{\alpha_\infty^n}\dot{\varepsilon}_{eff}^p \right) \qquad \text{(no summation over } n\text{)}$$

The reason for this generalization was to improve the large overestimate of ratcheting effects and to allow for a greater flexibility of the model. The isotropic

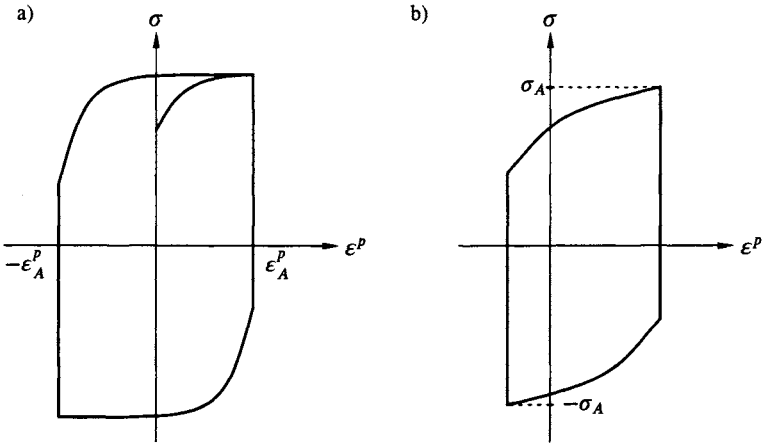

Figure 13.18: Kinematic hardening $m = 0$. a) symmetric strain cycling; b) symmetric stress cycling.

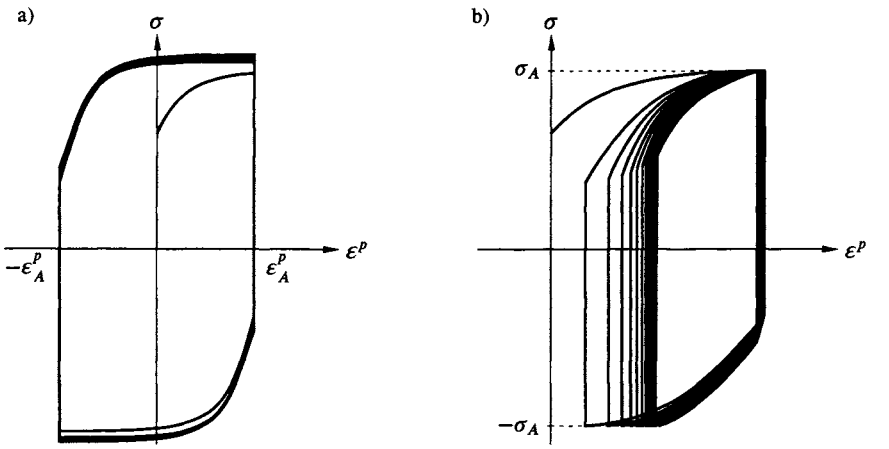

Figure 13.19: Mixed hardening $m = 0.3$. a) symmetric strain cycling; b) symmetric stress cycling.

hardening rule (13.71) could of course be generalized in the same way. Note that (13.87) can be viewed as a series expansion in exponential functions, i.e. in the limit it would be possible to include all types of curves within the model. Discussions of this generalization are also provided by Jiang and Kurath (1996).

Another improvement of the model also introduced by Chaboche *et al.* (1979) is to introduce a dependence between the saturated value of K, i.e. K_∞, and some measure of the maximum plastic strain amplitude, i.e. $K_\infty(\varepsilon^p_{ij}\varepsilon^p_{ij})$. It fol-

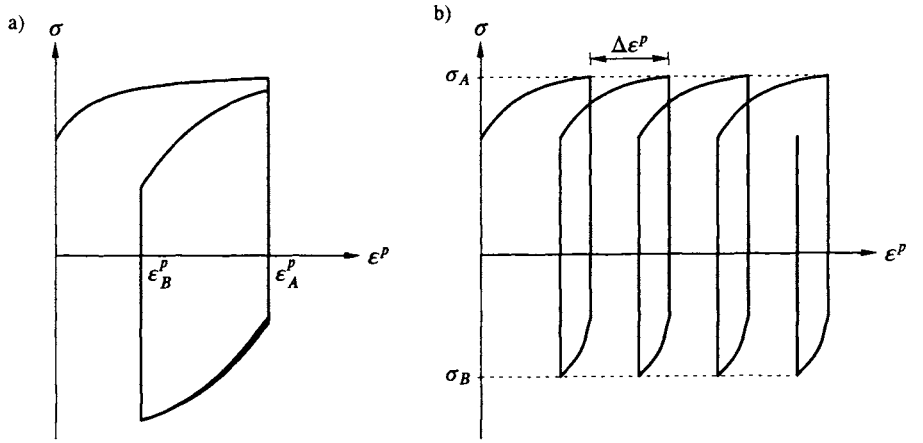

Figure 13.20: Kinematic hardening $m = 0$. a) unsymmetric strain cycling; b) unsymmetric stress cycling.

lows from the discussion above, that once we have reached the stabilized state for symmetric strain cycling, then in order to introduce additional isotropic hardening into the model K_∞ must vary with a quantity relating to the strain amplitude.

Returning to the mixed Armstrong-Frederick model considered previously, it is of interest to investigate whether this model implies that there exists a maximum range that limits the stress state. If this is the case, the yield surface must be at its maximum size and, in addition, also the back-stresses must be limited. According to (13.76), we then have

$$K = K_\infty \qquad \text{as well as} \qquad \dot{\alpha}_{ij} = 0$$

As $\dot{\varepsilon}^p_{eff} = \dot{\lambda}$, the last expression leads to

$$\dot{\varepsilon}^p_{ij} = \dot{\lambda}\frac{3}{2}\frac{\alpha_{ij}}{\alpha_\infty}$$

and a comparison with the flow rule (13.74) shows that

$$\bar{s}_{ij} = \frac{\bar{\sigma}_{eff}}{\alpha_\infty}\alpha_{ij}$$

In this expression, use of the yield criterion $f = 0$ with f given by (13.73) and observing that $K = K_\infty$ results in

$$\bar{s}_{ij} = \frac{\sigma_{yo} + K_\infty}{\alpha_\infty}\alpha_{ij} \qquad \text{i.e.} \qquad s_{ij} = (1 + \frac{\sigma_{yo} + K_\infty}{\alpha_\infty})\alpha_{ij} \tag{13.88}$$

Insertion of (13.88a) into the yield criterion $f = 0$ gives

$$\alpha_\infty = \alpha_{eff} \quad \text{where} \quad \alpha_{eff} = \left(\frac{3}{2}\alpha_{ij}\alpha_{ij}\right)^{1/2} \tag{13.89}$$

On the other hand, use of (13.88b) gives

$$\sigma_{eff} = \left(\frac{3}{2}s_{ij}s_{ij}\right)^{1/2} = \left(1 + \frac{\sigma_{yo} + K_\infty}{\alpha_\infty}\right)\alpha_{eff}$$

which with (13.89) implies

$$\boxed{\sigma_{eff,max} = \sigma_{yo} + \alpha_\infty + K_\infty} \tag{13.90}$$

where subscript 'max' is used to emphasize that this value of σ_{eff} is the largest possible value of the effective stress. This result agrees – as expected – with (13.84) when $\varepsilon^p_{eff} \to \infty$. The result (13.90) therefore represents a bounding surface as shown in Fig. 13.21.

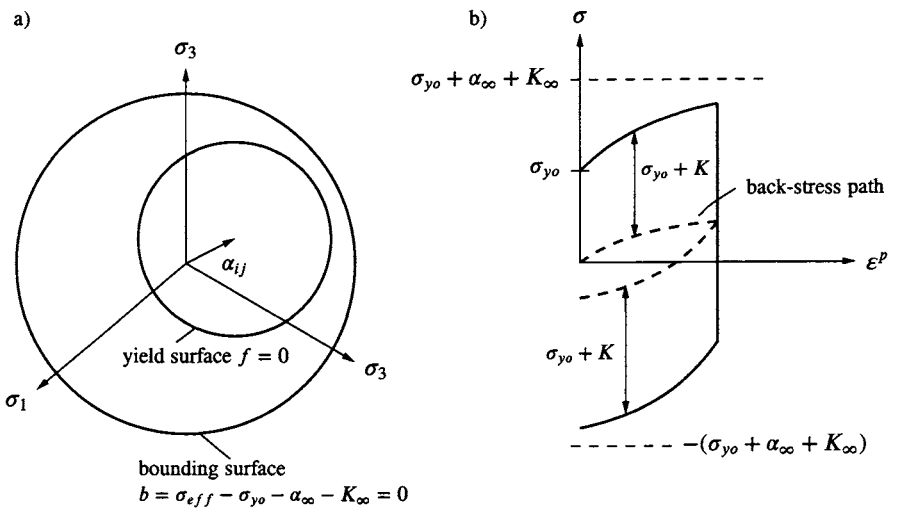

Figure 13.21: Mixed Armstrong-Frederick model with its bounding surface; a) deviatoric plane, b) uniaxial response.

The result (13.90) makes for an interesting interpretation of the Armstrong-Frederick model first pointed out by Marquis (1979) and also discussed by Chaboche (1989) and Jiang and Kurath (1996) namely that this model may be viewed also as a bounding surface model, i.e. a two-surface model, with Mróz' evolution law for the back-stresses α_{ij}.

To achieve this interpretation, isotropic hardening is ignored and the situation is then shown in Fig. 13.22. In the spirit of Mróz, the mapping stress s^M_{ij} is determined by O_bM being parallel to O_yP, i.e.

$$s^M_{ij} = a(s_{ij} - \alpha_{ij}) \tag{13.91}$$

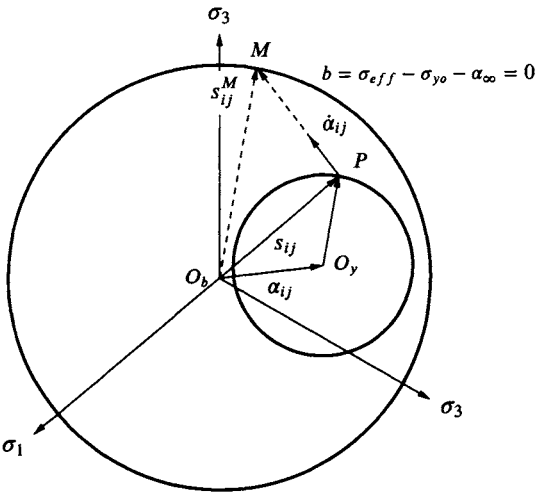

Figure 13.22: The Armstrong-Frederick evolution law for $\dot{\alpha}_{ij}$ viewed as Mróz evolution law.

where a is a positive proportionality factor. Since s_{ij}^M is located on the boundary surface defined by (13.90) and since isotropic hardening is ignored, we obtain

$$a\sqrt{\frac{3}{2}\bar{s}_{ij}\bar{s}_{ij}} = \sigma_{yo} + \alpha_\infty$$

Use of the yield condition $f = 0$ where f is defined by (13.73) gives

$$a = \frac{\sigma_{yo} + \alpha_\infty}{\sigma_{yo}}$$

Insertion of this expression into (13.91) results in

$$\alpha_{ij} = s_{ij} - \frac{\sigma_{yo}}{\sigma_{yo} + \alpha_\infty} s_{ij}^M \tag{13.92}$$

Use of the flow rule (13.74) in (13.76) with $m = 0$ gives

$$\dot{\alpha}_{ij} = h\left[\frac{s_{ij} - \alpha_{ij}}{\sigma_{yo}} - \frac{\alpha_{ij}}{\alpha_\infty}\right]\dot{\lambda}$$

Finally, insertion of (13.92) on the right-hand side provides

$$\dot{\alpha}_{ij} = \dot{\lambda}\frac{h}{\alpha_\infty}(s_{ij}^M - s_{ij})$$

This result is illustrated in Fig. 13.22 and it appears that we have recovered the evolution law of Mróz, cf. (13.12) and Fig. 13.10. The principal difference

between the two formulations is that in Mróz' model the plastic modulus is chosen to be constant (within each of the nested yield surfaces) and then the evolution law for the back-stress follows from the assumption that the active yield surface approaches the next yield surface so that no intersection occurs. In the Armstrong Frederick model, the evolution law for the back-stresses is directly postulated and the plastic modulus then turns out to vary in a realistic fashion; *a posteriori*, the Armstrong-Frederick model may then be interpreted as a two-surface model with a Mróz-type evolution law for the back-stresses.